STM JOURNALS

Journal of
Polymer & Composites

ISSN: 2321-2810 (Online)
ISSN: 2321-8525 (Print)
Volume 13, Special Issue 4, 2025
DOI (Journal): 10.37591/JoPC

https://journals.stmjournals.com/jopc

Review JoPC

Finite Element Formulation for Mechanical Buckling of FGM Plate Exposed to Various Boundary Conditions

Vineet Kumar [1,*], Pankaj Sonia[2]

Abstract

Mechanical buckling analysis of functionally graded (FG) material plates based on first-order shear deformation theory. In the real world many components manufactured by FG materials face the buckling load under certain conditions. Various types of gradation law for tailoring the material properties are applied by the researcher, out of that, presently a simple power law for material gradation is applied with shear correction factor (SCF) is used to take account of transverse shear & parabolic distribution of shear strain through z- direction of the plate. Every material has manufacturing defects at the time of production or preparation of material solutions. So, the need of simulation for the real materials based on porosity is required for factual results. In this direction there are two types of material porosities are modelled, and their effects are investigated viz. Tape I (even distributions of pores within plate) and Type II (Uneven distribution of pores). A four node iso-parametric element with five degrees of freedom at each node is used to discretize the plate element. Finite element technique in conjunction with Hamilton's principle is used to develop the governing equations and solutions. Validation studies are performed to verify and predict the accuracy of the present formulation. Results are presented in tabulated form as well as the parametric studies are done to explore the various dimensions taken into consideration. The slenderness ratio (a/b), aspect factor (a/h), material exponent index (p), various boundary conditions (BCs), uniaxial and biaxial buckling loading is explored and discussed.

Keywords: Finite element analysis, FG material, power law, mechanical buckling load, iso-parametric

INTRODUCTION

Functionally graded (FG) materials are the new advance composite materials whose properties are graded smoothly in three direction or in one direction microscopically to upgrade the structural strength. These materials propose, initially, for high thermal environment in the year of 1984. Japanese material scientist developed these materials for nuclear power plant where material can withstand high temperature environment with high strength[1]. FG materials are widely used in nuclear power plant, heat exchanger, civil engineering and mechanical engineering applications. FGMs make a difference from other composite materials which fail through a process called delamination in loading conditions. Kumar et al. [2–8] have been worked on FGM materials based on power law, exponential law and sigmoidal law.

Several studies have been conducted on the mechanical buckling analysis based on uniaxial and biaxial loading. Hosseini-Hashemi et al. [9] examined the exact solution of buckling analysis of isotropic plate with six type of boundary conditions. Mohammadi et al. [10] investigated the Lavy solution of functionally graded material plate for buckling analysis by applying the Kirchhoff plate theory. Ramu and Mohanty [11] estimated the

***Author for Correspondence**
Vineet Kumar

[1]Assistant professor, Department of Mechanical Engineering, Govt. Engineering College, Bikaner, Rajasthan, India
[2]Assistant professor, Department of Mechanical Engineering, GLA University, Mathura, Uttar Pradesh, India

Received Date: March 26, 2025
Accepted Date: April 30, 2025
Published Date: June 15, 2025

Citation: Vineet Kumar, Pankaj Sonia. Finite Element Formulation for Mechanical Buckling of FGM Plate Exposed to Various Boundary Conditions. Journal of Polymer & Composites. 2025; 13(Special Issue 4): S503–S513p.

© STM Journals 2025. All Rights Reserved

uniaxial and biaxial loading on rectangular FG material plate using classical plate theory (CPT). The simply supported FG plate is discretized by finite element method accompanied with power law gradation method. Further, shear deformation theory is utilized to obtain the solution and in the same line, Kumar et al. [12] applied the first-order shear deformation theory to obtain the solution of buckling analysis of FGM tapered plate using semi-analytical method. Kim and Thai [13] developed the closed form solution based on third order shear deformation theory for buckling analysis. Neutral surface position was investigated by decoupling the governing equations of P-FGM plate. It was also assumed that plate was rested on Pasternak's foundation. Prakash et al. [14] investigated the non-linear behaviour of buckling response of FGM plate under in-plane load conditions. Asemi et al. [15] carried out the solution for uniaxial, biaxial and shear compression induced buckling of FGM rectangular plate. Various mode shape of buckling response was investigated using three-dimensional approach for rectangular plate in conjunction with Finite element method. Uymaz and Aydogdu [16] developed the 3-D elasticity and higher-order plate theory based solution for shear buckling analysis. Afzali et al. [17] carried out the solution of thermal buckling analysis of rectangular FGM plate using Carrera Unified Formulation.

Further, materials with changing composition by porosities of structure are field of interest for the researchers. Modelling of porosities is designed to change the microstructural properties of the materials which may be beneficial to improve the various characteristics. In order to this, Rezaei and Saidi [18] investigated the exact solution of vibration analysis of porous structures. Third order shear deformation theory was applied for the plate supported with various boundary conditions. Kumar et al. [19] investigated the vibration response analysis of porous tapered plate using Galerkin's Vlasov method. The porous tapered plate was assumed to be rested on Pasternak's elastic foundation. Barati et al. [20] examined the buckling analysis of functionally graded piezoelectric plate using refined four variable plate theory. In view of above, the purpose of the present work is to form a finite element model of porous FG materials plate for buckling analysis. The simple framework of FSDT is adopted to perform various analysis based on different boundary conditions. An iso-parametric formulation of four node rectangular element with five degree of freedom is used to uniaxial and biaxial compression.

GEOMETRY OF POROUS PLATE

The FG material plate structure concerns a domain -h/2 to h/2 with h its uniform thickness and its mid plane having the dimension a x b as depicted in Figure 1 (a). The plate material is assumed to be functionally graded and the variation of Young's modulus in thickness direction is shown in Fig. 1 (b). In addition, it was considered that plate structure has two types of porosity within it and the effect of voids on the Young's modulus illustrated in Fig.1(c-d). Two types of loading conditions for buckling analysis are considered in the present article and shown in Figure 2. Simple power law is applied to tailor the material in the thickness direction.

$$E(z) = E_t + \left(E_t - E_b\right)V_m,\ V_t = \left(1/2 + z/h\right)^p, \qquad -h/2 \le z \le h/2,\ V_t + V_m = 1$$

Where, E_t, E_b are the elastic modulus at the top and bottom surface, while V_t, V_m are the volume fraction of ceramic and metallic constituents materials. Two different types of porosity [21] can be discribe as,

$$\text{Type I, } E(z) = E_t + \left(E_t - E_b\right)V_m - e/2\left(E_t + E_b\right) \tag{1}$$

$$\text{Type II, } E(z) = E_t + \left(E_t - E_b\right)V_m - e/2\left(E_t + E_b\right)\left(1 - \frac{2|z|}{h}\right) \tag{2}$$

© STM Journals 2025. All Rights Reserved

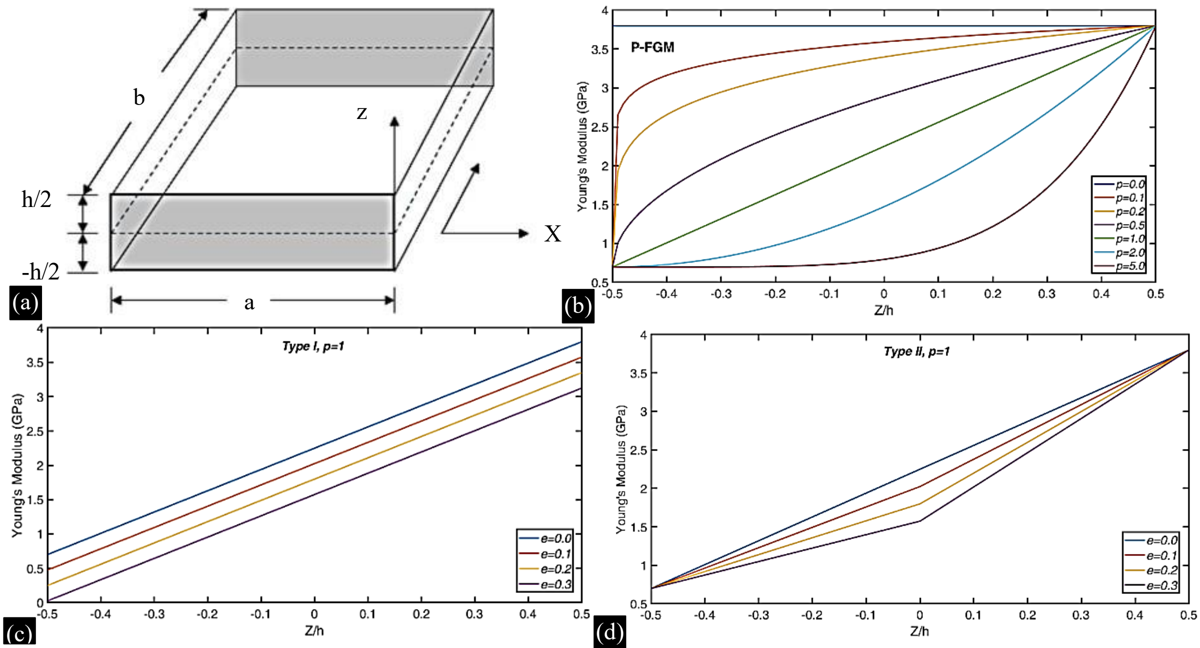

Figure 1. Al_2O_3/Al materials FGM plate (a) geometry of plate (b) Power- law function (c) Type I porous plate and, (d) Type II porous plate.

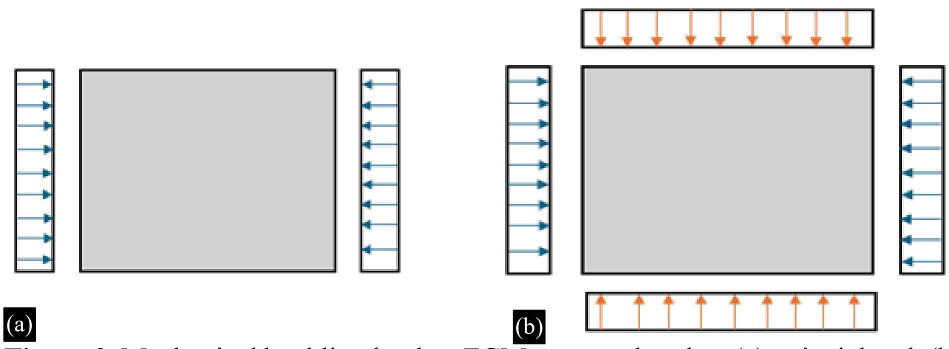

Figure 2. Mechanical buckling load on FGM rectangular plate (a) uniaxial and, (b) biaxial compression.

DEVELOPMENT OF GOVERNING EQUATION

Displacement components u, v, and w along x, y, and z directions, respectively, first order shear deformation plate theory is applied [22].

$$\begin{Bmatrix} u \\ v \\ w \end{Bmatrix} = \begin{Bmatrix} u_0 \\ v_0 \\ w_0 \end{Bmatrix} + z \begin{Bmatrix} \phi_x \\ \phi_y \\ 0 \end{Bmatrix} \tag{3}$$

$$\begin{Bmatrix} \varepsilon_{xx} \\ \varepsilon_{yy} \\ \gamma_{xy} \end{Bmatrix} = \begin{Bmatrix} u_{0,x} \\ v_{0,y} \\ u_{0,y} + v_{0,x} \end{Bmatrix} + z \begin{Bmatrix} \phi_{x,x} \\ \phi_{y,y} \\ \phi_{x,y} + \phi_{y,x} \end{Bmatrix} \tag{4}$$

$$\{\varepsilon\} = \{\varepsilon_m\} + z\{\varepsilon_b\} \tag{5}$$

$$\begin{Bmatrix} \gamma_{xz} \\ \gamma_{yz} \end{Bmatrix} = \begin{Bmatrix} w_{0,x} + \phi_x \\ w_{0,y} + \phi_y \end{Bmatrix} = \{\gamma\} \tag{6}$$

© STM Journals 2025. All Rights Reserved

$$\begin{Bmatrix}\sigma_{xx}\\ \sigma_{yy}\\ \tau_{xy}\end{Bmatrix}=\begin{bmatrix}A_{11} & A_{12} & 0\\ A_{12} & A_{22} & 0\\ 0 & 0 & A_{66}\end{bmatrix}\begin{Bmatrix}\varepsilon_{xx}\\ \varepsilon_{yy}\\ \gamma_{xy}\end{Bmatrix}\qquad \begin{Bmatrix}\tau_{xz}\\ \tau_{yz}\end{Bmatrix}=k_s\begin{bmatrix}A_{44} & 0\\ 0 & A_{55}\end{bmatrix}\begin{Bmatrix}\gamma_{xz}\\ \gamma_{yz}\end{Bmatrix} \tag{7}$$

$$A_{11}=A_{22}=\frac{E(z)}{1-\upsilon^2};\quad A_{12}=\upsilon\frac{E(z)}{1-\upsilon^2};\quad A_{44}=A_{55}=A_{66}=\frac{E(z)}{2(1+\upsilon)} \tag{8}$$

$$Q=\begin{Bmatrix}\sigma_{xx}\\ \sigma_{yy}\\ \tau_{xy}\end{Bmatrix},\qquad Q_s=\begin{Bmatrix}\tau_{xz}\\ \tau_{yz}\end{Bmatrix} \tag{9}$$

In the present work, the Hamilton's principle is used here to derive the governing equation.

$$\int_{t_1}^{t_2}(\delta U+\delta V)dt=0 \tag{10}$$

The variation in the strain energy is presented as,

$$\delta U=\int_{\Omega}\left(\sigma_{xx}\delta\varepsilon_{xx}+\sigma_{yy}\delta\varepsilon_{yy}+\tau_{xy}\delta\gamma_{xy}+\tau_{xz}\delta\gamma_{xz}+\tau_{yz}\delta\gamma_{yz}\right)d\Omega \tag{11}$$

$$\delta U=\int_{A}\left(N_{xx}\delta\varepsilon_{xx}^{m}+N_{yy}\delta\varepsilon_{yy}^{m}+N_{xy}\delta\gamma_{xy}^{m}+M_{xx}\delta\varepsilon_{xx}^{b}+M_{yy}\delta\varepsilon_{yy}^{b}+M_{xy}\delta\tau_{xy}^{b}+Q_{xz}\delta\gamma_{xz}^{m}+Q_{yz}\delta\gamma_{yz}^{m}\right)dA \tag{12}$$

$$\begin{Bmatrix}N_{xx}\\ N_{yy}\\ N_{xy}\end{Bmatrix}=\int_{-h/2}^{h/2}\begin{Bmatrix}\sigma_{xx}\\ \sigma_{yy}\\ \tau_{xy}\end{Bmatrix}dz,\qquad \begin{Bmatrix}M_{xx}\\ M_{yy}\\ M_{xy}\end{Bmatrix}=\int_{-h/2}^{h/2}\begin{Bmatrix}\sigma_{xx}\\ \sigma_{yy}\\ \tau_{xy}\end{Bmatrix}zdz,\quad \begin{Bmatrix}Q_{xz}\\ Q_{yz}\end{Bmatrix}=\int_{-h/2}^{h/2}\begin{Bmatrix}\tau_{xz}\\ \tau_{yz}\end{Bmatrix}dz, \tag{13}$$

Inplane compressive load may be obtained as,

$$\delta V=\int_{A}\left(\sigma^{0}\right)^{T}\delta\varepsilon\ \ dA,\ \sigma^{0}=\begin{bmatrix}\sigma_{xx}^{0} & \tau_{xy}^{0}\\ \tau_{xy}^{0} & \sigma_{yy}^{0}\end{bmatrix} \tag{14}$$

After substitution of displacement field into strain based equations, we get the following expression,

$$\delta V=\int_{A}\left(\nabla w^{T}\sigma^{0}\nabla w\right)\ dA\text{, Where, }\nabla=\{\partial/\partial x,\partial/\partial y\}^{T} \tag{15}$$

Resulting total potential energy converting into the eigen value problem,

$\left([K]+\left[K_g\right]\right)\{d_i\}=0$, where, K,K_g are the stiffness and geometric stiffness matrix respectively.

$\left|[K]-\lambda\left[K_g\right]\right|=0$, and critical buckling load can be defined as, $N_{cr}=\lambda_{cr}N$ where N is applied load.

Now, the plate is discritized into number of quadrilateral element and each element contains four corner as dipicted in Figure 3. The isoparametric element was chosen for five degree of freedom at each node. Lagrange shape functions at each node for linear element is defined as:

$N_a(\xi,\eta)=1/4(1-\xi)(1-\eta),\ N_b(\xi,\eta)=1/4(1+\xi)(1-\eta),\ N_c(\xi,\eta)=1/4(1+\xi)(1+\eta),N_d(\xi,\eta)=1/4(1-\xi)(1+\eta)$

The generalized displacement vector may be specified as, $d_i=\sum_{i=1}^{4}N_i d_i$,

© STM Journals 2025. All Rights Reserved

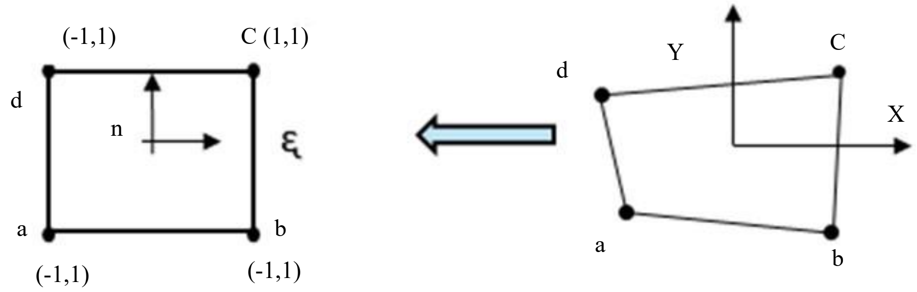

Figure 3. Four node element with corosponding degree of freedom.

Table 1. Convergence test for uniaxial buckling load ($\lambda_{cr} = Nb^2 / E_C h^3$) of FGM plate.

Mesh size	Results
8x8	5.1660
16x16	4.6570
24x24	4.5831
32x32	4.5589
36x36	4.5525
40x40	4.5480

Table 2. Comparison of uniaxial and biaxial mechanical buckling ($\lambda_{cr} = Nb^2 / Eh^3$) responses.

a/h	Uniaxial	Bi axial	Results
50	3.6104	1.8052	Present
	3.6071	1.8036	Kim et al.[23], FSDT
	3.5975	1.7988	Rouzegar and Sharifpoor [24], RPT
100	3.6165	1.8082	Present
	3.6132	1.8066	Kim et al.[23], FSDT
	3.6036	1.8018	Rouzegar and Sharifpoor [24], RPT

CONVERGENCE AND VALIDATION STUDY

The mesh convergence test is executed to find the ideal mesh size in terms of elements selection in the plates. It can be seen in Table 1, results are converging at a specific values of mesh size and this is done for a fully clamped square FGM plate with aspect factor a/h=100 & material exponent index *p*=1. The material properties of FG (Al_2O_3/Al) materials as follows, Young's modulus for Al_2O_3 & Al is taken 380 & 70 GPa and Poisson's ratio is chosen as 0.3 for both the materials. Mesh size 40x40 is adopted uniformly for all results sections in the article with SCF 5/6.

Here, a first order shear deformation theory is used to investigate the mechanical buckling response of FGM plates. So, several studies have been conducted to validate the present formulation for accuracy and efficacy. The first comparison study is done for square isotropic plate with simply supported boundary condition and different span ratios. Kim et al. [23] applied the two variable refined plate theory with Navier solution technique and Rouzegar & Sharifpoor [24] used the finite element technique to obtained the solution of isotopic plate in Table 2.

In Table 3. Results are compared for the effect of slenderness (a/b) and aspect ratios (a/h) on critical buckling load of simply supported FGM plate. The present results have quite close agreement with results published by Zenkour and Aljadani [25] using refined higher-order shear and normal deformation plate theory. In addition, Navier's procedure is applied, in published results, to obtain the buckling behavior of simply supported plate made of Al_2O_3/Al materials. Material exponent index (*p*) 0,1,5 & 10 are taken to investigate the uniaxial and biaxial mechanical buckling loads.

© STM Journals 2025. All Rights Reserved

Table 3. Comparison of uniaxial & biaxial mechanical buckling load ($\lambda_{cr} = Na^2 / E_m h^3$) for various slenderness ratio and aspect factors of P-FGM plate structure.

Slenderness ratio (a/b)	**Aspect factor (a/h)**	**Uniaxial mechanical buckling**				**Source**
		***p*=0**	***p* =1**	***p* =5**	***p* =10**	
0.5	50	7.6629	3.8200	2.5202	2.2949	Present
		7.6554	3.8166	2.5171	2.2922	Ref. [25]
	100	7.6710	3.8234	2.5229	2.2977	Present
		7.6635	3.8200	2.5204	2.2956	Ref. [25]
1	50	19.5991	9.7715	6.4456	5.8688	Present
		19.5814	9.7636	6.4372	5.8613	Ref. [25]
	100	19.6323	9.7855	6.4568	5.8804	Present
		19.6145	9.7775	6.4507	5.8751	Ref. [25]
a/b	a/h	Bi-axial mechanical buckling				
		p =0	*p* =1	*p* =5	*p* =10	
0.5	50	6.1303	3.0560	2.0161	1.8359	Present
		6.1243	3.0533	2.0137	1.8338	Ref. [25]
	100	6.1368	3.0587	2.0183	1.8382	Present
		6.1308	3.0560	2.0163	1.8365	Ref. [25]
1.5	50	15.9023	7.9302	5.2296	4.7608	Present
		15.8875	7.9235	5.2212	4.7530	Ref. [25]
	100	15.9460	7.9485	5.2444	4.7760	Present
		15.9311	7.9419	5.2389	4.7712	Ref. [25]

Next, present results are compared by Wu et al.[26] for fully clamped FGM plate, made of Al_2O_3/Al materials, with shear correction factor 5/6 in Table 4. The simple power law, for material gradation, is applied to investigate the uniaxial buckling load by choosing material exponent index as *p*= 0,1,2 & 5 with plate aspect factor a/h=100. Wu et al. [26] used the FSDT with Von-Karman nonlinear displacement field and obtained the solution by analytical method. Table 5, compared the results by Gupta and Kumar [27] for porous FGM plate with different slenderness ratio (a/h)= 50 & 100, material exponent index *p*=0.5, porosity parameter (Type II) *e* = 0, 0.1, 0.3 & 0.5 and aspect factor a/b=1. Although, there is negligible variation in the present results, it may be due to the differences between present plate theory (FSDT) and higher-order plate theory used for already published results.

Table 4. Comparison of uniaxial compressive buckling ($\lambda_{cr} = Nb^2 / E_C h^3$) results for fully clamped FGM plate.

***p* =0**	***p* =1**	***p* =2**	***p* =5**	**Source**
9.1222	4.5480	3.5489	3.0000	Present
9.1579	4.6158	3.5789	3.0342	Ref. [26]

Table 5. Comparison of uniaxial buckling ($\lambda_{cr} = Na^2 / E_m h^3$) results for SSSS porous (Type II) FGM plate.

a/h	***e* =0**	***e* =0.1**	***e* =0.3**	***e* =0.5**	**Source**
50	12.7067	12.3756	11.7023	11.0101	Present
	13.5202	13.0430	12.4240	11.7968	Ref. [27]
100	12.7258	12.3946	11.7208	11.0282	Present
	13.3834	13.0762	12.4573	11.8306	Ref. [27]

© STM Journals 2025. All Rights Reserved

RESULTS AND DISCUSSION

Based on FSDT, the equation of motion for finite element model, which is employed for uniaxial and biaxial buckling analysis of FGM plate, is developed from Hamilton's principle. Al_2O_3/Al material of FG constituents is used for finding new results in the present work. By default, non-dimensional results for buckling analysis are obtained by the non-dimensional parameter $\lambda_{cr} = Na^2 / E_m h^3$. Table 6, depicted the uniaxial buckling results for porous (Type I) FG materials plate. The two-material exponent index *p*=0.5 & 1 along with three porosity parameters *e* =0, 0.1 & 0.3 is selecting for first four mode of buckling response. There are two slenderness ratio a/b =0.5 & 1 of FG plate for each boundary conditions i.e. simply supported & fully clamped respectively. It was observed that on increase of material exponent index, buckling load is decreased irrespective of boundary conditions. The reason is quite clear that on increase of material exponent index, stiffness decreases of the materials. Secondly, on increase of porosity parameter (more voids) buckling load decreases and it may be due to reduction in stiffness of the materials. Next observation is regarding the slenderness ratio, as the slenderness ratio increases, buckling load increases. Moreover, buckling load increases on increase of boundary constraints as we can see, the buckling load is more in case of fully clamped boundary conditions.

Results based on Type II porosity are shown in Table 7, the pattern of the finding are similar as in case of Type I porosity model. Furthermore, Table 8, contains the results for biaxial compression of slenderness ratio a/b=1.5 plate with 0,0.1,1,2 & 5 materials exponent index. Both types of porosity model were considered during the buckling analysis. It was seen that critical buckling load was higher for porosity Type II model for almost material exponent index 0.1,1,2 & 5. It was a similar pattern for SSSS and CCCC boundary conditions. It may be concluded that on the increase of ceramic constituents, eigen value increases which reflects the more buckling load.

Table 6. Uniaxial buckling load of porous (Type I) FG material plate with thickness h=0.01,

B, Cs	a/b	Mode	*p*=0.5			*p*=1		
			e=0	*e=0.1*	*e=0.2*	*e=0*	*e=0.1*	*e=0.2*
SSSS	0.5	I	4.9723	4.4850	3.9912	3.8234	3.2893	2.7353
		II	12.7535	11.5036	10.2372	9.8068	8.4371	7.0161
		III	14.4019	12.9906	11.5607	11.0746	9.5280	7.9237
		IV	19.9282	17.9754	15.9969	15.3244	13.1844	10.9645
	1	I	12.7258	11.4787	10.2150	9.7855	8.4187	7.0009
		II	19.9123	17.9610	15.9841	15.3121	13.1739	10.9557
		III	35.5345	32.0532	28.5259	27.3271	23.5123	19.5549
		IV	50.9648	45.9713	40.9120	39.1924	33.7205	28.0440
CCCC	0.5	I	15.4192	13.9083	12.3773	11.8569	10.2012	8.48340
		II	25.7670	23.2422	20.6840	19.8145	17.0477	14.1774
		III	28.2220	25.4570	22.6556	21.7034	18.6735	15.5304
		IV	34.8849	31.4673	28.0045	26.8277	23.0827	19.1976
	1	I	32.1054	28.9598	25.7726	24.6893	21.2422	17.6662
		II	37.0816	33.4490	29.7683	28.5174	24.5368	20.4073
		III	62.5541	56.4276	50.2204	48.1110	41.3982	34.4341
		IV	79.4182	71.6402	63.7596	61.0816	52.5591	43.7176

Table 7. Uniaxial buckling of porous (Type II) FG material plate with thickness h=0.01,

B, Cs	a/b	Mode	*p*=0.5			*p*=1		
			e=0	*e=0.1*	*e=0.2*	*e=0*	*e=0.1*	*e=0.2*
SSSS	0.5	I	4.9723	4.8429	4.7120	3.8234	3.6720	3.5165
		II	12.7535	12.4215	12.0860	9.8068	9.4185	9.0195
		III	14.4019	14.0269	13.6478	11.0746	10.6361	10.1854
		IV	19.9282	19.4093	18.8847	15.3244	14.7176	14.0939
	1	I	12.7258	12.3946	12.0597	9.7855	9.3981	8.9999
		II	19.9123	19.3937	18.8696	15.3121	14.7058	14.0826
		III	35.5345	34.6084	33.6724	27.3271	26.2447	25.1323
		IV	50.9648	49.6370	48.2949	39.1924	37.6402	36.0450
CCCC	0.5	I	15.4192	15.0177	14.6119	11.8569	11.3875	10.9050
		II	25.7670	25.0959	24.4176	19.8145	19.0298	18.2234
		III	28.2220	27.4866	26.7432	21.7034	20.8438	19.9603
		IV	34.8849	33.9757	33.0567	26.8277	25.7650	24.6729
	1	I	32.1054	31.2691	30.4236	24.6893	23.7115	22.7066
		II	37.0816	36.1151	35.1381	28.5174	27.3878	26.2268
		III	62.5541	60.9221	59.2725	48.1110	46.2044	44.2452
		IV	79.4182	77.3463	75.2519	61.0816	58.6610	56.1735

Table 8. Biaxial buckling for porous (Type I & Type II) FG materials plate with slenderness ratio (a/b) =1.5 and h=0.01.

B, Cs	*p*	Type I			Type II		
		e =0	*e =0.1*	*e =0.2*	*e =0*	*e =0.1*	*e =0.2*
SSSS	0	15.946	15.0019	14.0577	15.946	14.3699	15.4735
	0.1	14.3699	13.4213	12.4721	14.3699	14.1315	13.8930
	1	7.9485	6.8385	5.6869	7.9485	7.6338	7.3104
	2	6.2025	4.9692	3.6345	6.2025	5.8319	5.4412
	5	5.2444	3.9809	2.5297	5.2444	4.8648	4.4527
CCCC	0	45.5202	42.8250	40.1297	45.5202	44.8444	44.1684
	0.1	41.0233	38.3154	35.6057	41.0233	40.3415	39.6592
	1	22.6978	19.5294	16.2424	22.6978	21.7987	20.8747
	2	17.7113	14.1918	10.3824	17.7113	16.6529	15.5374
	5	14.9700	11.3649	7.2246	14.9700	13.8858	12.7090

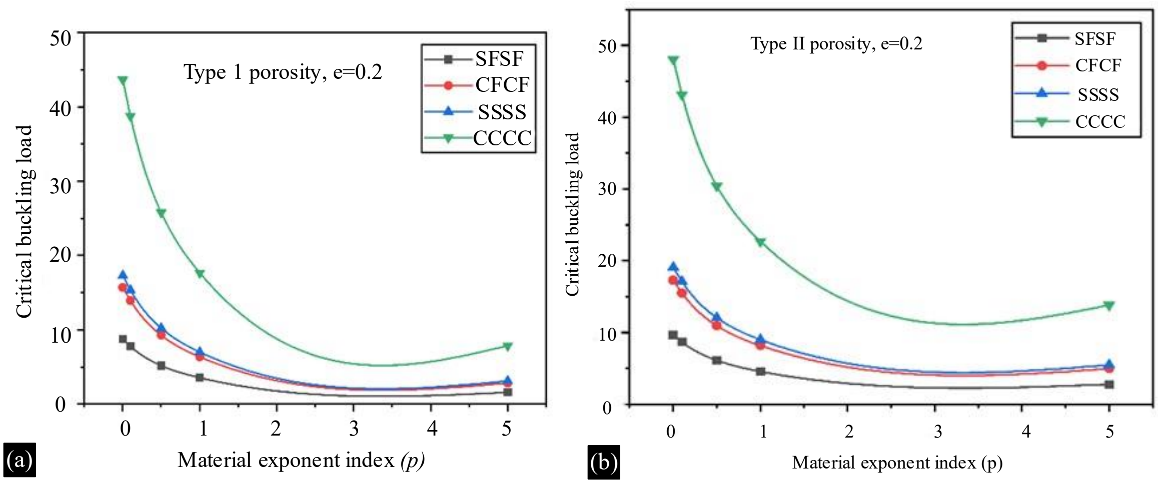

Figure 4. Comparison of two porosity models for uniaxial load with different BC's (a) Type I and, (b) Type II.

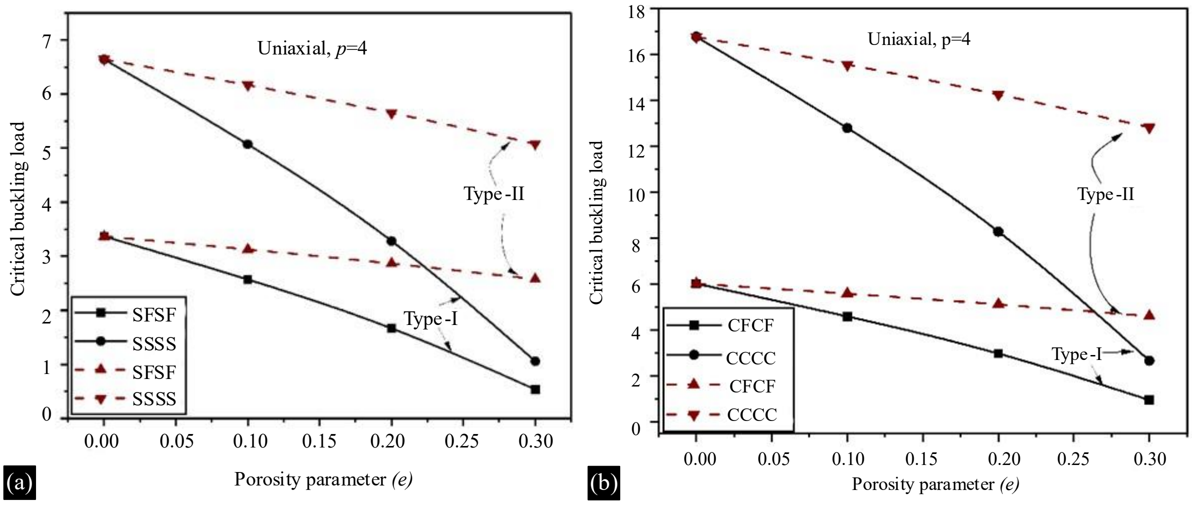

Figure 5. Comparison of boundary conditions with porosity (a) SFSF & SSSS and, (b) CFCF & CCCC. (a) a/b=1, p=4 (b) a/b=1, p=4

A parametric study was done for two porosity models with slenderness ratio a/h=100 of square FG material plate supported on various boundary conditions viz; SFSF, CFCF, SSSS and CCCC, as illustrated in Figure 4 (a-b). One interesting thing found, when we compare both porosity models, it seems that critical buckling load was higher in case of Type II porosity model for respective each boundary conditions. Next observation was found that the sequence of increasing buckling load based on the boundary conditions as SFSF <CFCF<SSSS<CCCC. Figure 5 (a) shows the comparison between SFSF & SSSS BCs for type I & Type II porosity model with different set of porosity parameters. It was observed that on increase of porosity parameters, a continuous decrease in critical buckling load was observed for Type I porosity model while decreasing trend for Type II porosity model was small in comparison with Type I model. Similar trends were observed for CFCF & CCCC BCs in Figure.5 (b).

CONCLUSIONS

The finite element method has been employed to determine the critical buckling loads of functionally graded plates based on the first-order shear deformation theory. The present method contains the four node quadrilateral elements with five degree of freedom and a shear correction factor is applied to accommodate the transverse shear strain through thickness direction. Different boundary constraints, slenderness ratio, aspect factor and material exponent index for FG plates are examined. Two different types of porosity model are applied to show the effect of voids present in FG structures. It is seen that the ceramic constituents increase in the FG plate i.e. the eigen value increases, the critical buckling loads increase. And in the similar fashion, on increase of porosity parameter (increase of voids), critical buckling load decreases.

REFERENCES

1. Koizumi, M.: FGM activities in Japan. Compos. Part B Eng. 28, 1–4 (1997). https://doi.org/10.1016/S1359-8368(96)00016-9
2. Kumar, V., Singh, S.J., Saran, V.H., Harsha, S.P.: An analytical framework for rectangular FGM tapered plate resting on the elastic foundation. Mater. Today Proc. 28, 1719–1726 (2020). https://doi.org/10.1016/j.matpr.2020.05.136
3. Kumar, V., Singh, S.J., Saran, V.H., Harsha, S.P.: Vibration analysis of the rectangular FG materials plate with variable thickness on Winkler-Pasternak-Kerr elastic foundation. Mater. Today Proc. 62, 184–190 (2022). https://doi.org/10.1016/j.matpr.2022.02.615
4. Kumar, V., Singh, S.J., Saran, V.H., Harsha, S.P.: Vibration response of exponentially graded plates on elastic foundation using higher-order shear deformation theory. Indian J. Eng. Mater. Sci. 29, 181–188 (2022)

© STM Journals 2025. All Rights Reserved

5. Kumar, V., Singh, S.J., Harsha, S.P.: Temperature-Dependent Vibration Characteristics of Porous FG Material Plates Utilizing FSDT. Int. J. Struct. Stab. Dyn. 24, 1–35 (2023). https://doi.org/10.1142/S021945542450072X
6. Kumar, V., Singh, S.J., Saran, V.H., Harsha, S.P.: Vibration response of the exponential functionally graded material plate with variable thickness resting on the orthotropic Pasternak foundation. Mech. Based Des. Struct. Mach. (2023). https://doi.org/10.1080/15397734.2023.2193623
7. Kumar, V., Singh, S.J., Saran, V.H., Harsha, S.P.: Vibration characteristics of porous FGM plate with variable thickness resting on Pasternak's foundation. Eur. J. Mech. A/Solids. 85, 104124 (2021). https://doi.org/10.1016/j.euromechsol.2020.104124
8. Kumar, V., Singh, S.J., Saran, V.H., Harsha, S.P.: Exact solution for free vibration analysis of linearly varying thickness FGM plate using Galerkin-Vlasov's method. Proc. Inst. Mech. Eng. Part L J. Mater. Des. Appl. (2020). https://doi.org/10.1177/1464420720980491
9. Hosseini-Hashemi, S., Khorshidi, K., Amabili, M.: Exact solution for linear buckling of rectangular Mindlin plates. J. Sound Vib. 315, 318–342 (2008). https://doi.org/10.1016/j.jsv.2008.01.059
10. Mohammadi, M., Saidi, A.R., Jomehzadeh, E.: Levy solution for buckling analysis of functionally graded rectangular plates. Appl. Compos. Mater. 17, 81–93 (2010). https://doi.org/10.1007/s10443-009-9100-z
11. Ramu, I., Mohanty, S.C.: Buckling Analysis of Rectangular Functionally Graded Material Plates under Uniaxial and Biaxial Compression Load. Procedia Eng. 86, 748–757 (2014). https://doi.org/10.1016/j.proeng.2014.11.094
12. Kumar, V., Singh, S.J., Saran, V.H., Harsha, S.P.: Effect of elastic foundation and porosity on buckling response of linearly varying functionally graded material plate. Structures. 55, 1186–1203 (2023). https://doi.org/10.1016/j.istruc.2023.06.084
13. Thai, H.T., Kim, S.E.: Closed-form solution for buckling analysis of thick functionally graded plates on elastic foundation. Int. J. Mech. Sci. 75, 34–44 (2013). https://doi.org/10.1016/j.ijmecsci.2013.06.007
14. Prakash, T., Singha, M.K., Ganapathi, M.: Influence of neutral surface position on the nonlinear stability behavior of functionally graded plates. Comput. Mech. 43, 341–350 (2009). https://doi.org/10.1007/s00466-008-0309-8
15. Asemi, K., Shariyat, M., Salehi, M., Ashrafi, H.: A full compatible three-dimensional elasticity element for buckling analysis of FGM rectangular plates subjected to various combinations of biaxial normal and shear loads. Finite Elem. Anal. Des. 74, 9–21 (2013). https://doi.org/10.1016/j.finel.2013.05.011
16. Uymaz, B., Aydogdu, M.: Three dimensional shear buckling of FG plates with various boundary conditions. Compos. Struct. 96, 670–682 (2013). https://doi.org/10.1016/j.compstruct.2012.08.031
17. Afzali, M., Farrokh, M., Carrera, E.: Thermal buckling loads of rectangular FG plates with temperature-dependent properties using Carrera Unified Formulation. Compos. Struct. 295, (2022). https://doi.org/10.1016/j.compstruct.2022.115787
18. Rezaei, A.S., Saidi, A.R.: Exact solution for free vibration of thick rectangular plates made of porous materials. Compos. Struct. 134, 1051–1060 (2015). https://doi.org/10.1016/j.compstruct.2015.08.125
19. Kumar, V., Singh, S.J., Saran, V.H., Harsha, S.P.: Vibration Response Analysis of Tapered Porous FGM Plate Resting on Elastic Foundation. Int. J. Struct. Stab. Dyn. 2350024, 1–31 (2022). https://doi.org/10.1142/S0219455423500244
20. Barati, M.R., Sadr, M.H., Zenkour, A.M.: Buckling analysis of higher order graded smart piezoelectric plates with porosities resting on elastic foundation. Int. J. Mech. Sci. 117, 309–320 (2016). https://doi.org/10.1016/j.ijmecsci.2016.09.012
21. Dhuria, M., Grover, N., Goyal, K.: Influence of porosity distribution on static and buckling responses of porous functionally graded plates. Structures. 34, 1458–1474 (2021). https://doi.org/10.1016/j.istruc.2021.08.050
22. J.N. Reddy: Theory and Analysis of Elastic Plate and Shells. (2009)

© STM Journals 2025. All Rights Reserved

23. Kim, S.E., Thai, H.T., Lee, J.: Buckling analysis of plates using the two variable refined plate theory. Thin-Walled Struct. 47, 455–462 (2009). https://doi.org/10.1016/j.tws.2008.08.002
24. Rouzegar, J., Sharifpoor, R.A.: Finite element formulations for buckling analysis of isotropic and orthotropic plates using two-variable refined plate theory. Iran. J. Sci. Technol. - Trans. Mech. Eng. 41, 177–187 (2017). https://doi.org/10.1007/s40997-016-0055-z
25. Zenkour, A.M., Aljadani, M.H.: Mechanical buckling of functionally graded plates using a refined higher-order shear and normal deformation plate theory. Adv. Aircr. Spacecr. Sci. 5, 615–632 (2018). https://doi.org/10.12989/aas.2018.5.6.615
26. Wu, T.L., Shukla, K.K., Huang, J.H.: Post-buckling analysis of functionally graded rectangular plates. Compos. Struct. 81, 1–10 (2007). https://doi.org/10.1016/j.compstruct.2005.08.026
27. Gupta, A.K., Kumar, A.: Buckling Analysis of Porous Functionally Graded Plates. Eng. Technol. Appl. Sci. Res. 13, 10901–10905 (2023). https://doi.org/10.48084/etasr.5943